Combined use of High-Speed Videography and PDV Profilometry for Measuring High Speeds Flyers and Impact Shock Dynamics

B. Thurston[1,*], M. Abdelmaola[1], J. Seidt[2], A. Gilat[2], A. Vivek[1], G. S. Daehn[1]

[1] Department of Materials Science and Engineering, The Ohio State University, USA
[2] Department of Mechanical and Aerospace Engineering, The Ohio State University, USA
*Corresponding author. Email: Thurston.56@osu.edu

Abstract

Challenges remain in understanding the dynamic forces that occur with small scale explosive detonations and the subsequent impact those forces have on flyer velocity and deformation profiles. This work presents two data acquisition techniques for probing the behavior of various materials disturbed by laser induced detonations. The physical reactions of metallic flyers and transparent acrylic are cataloged and measured. The data acquisition techniques described here are high speed videography, Photon Doppler Velocimetry Profilometry (usually referred to as PDV Profilometry). High-speed videography provides a detailed temporal view of shock wave propagation, impact pressure distribution, and plasma plume dynamics. A Shimadzu Hypervision HPV-X2 camera was used at up to 10 million frames per second. For nanosecond scale velocity measurements PDV Profilometry was used to capture flyer velocity, acceleration, and deformation. PDV profilometry is a relatively new technique, here its ability to collect 8 or more velocity profiles at up to 750 km/s from a single PDV probe is demonstrated. Measurements of a shock front induced by the collision of a super sonic flyer against the surface of an acrylic cube is observed using the high speed camera. In this acrylic collision experiment impact and shock speeds up to 10km/s are recorded. Combining these techniques, a wide variety of experiments may be undertaken and observed with remarkable clarity in the nanosecond to microsecond time domain.

Keywords

Transient impact pressure, Pressure attenuation, Shock wave, Augmented laser impact Process, Photon Doppler Velocimetry (PDV), PDV Profilometry, High Speed Imaging

1 Introduction

Measurement techniques, for high-speed phenomena often suffer from a tradeoff between spatial and temporal resolution and often do not provide direct visualization of shock induced phenomena (Watts and Tassel, 1989), (Elkarous et al., 2016). In this study, two techniques for measuring highly transient shock induced phenomena with both good spatial and temporal resolution, high-speed videography and Photon Doppler Velocimetry Profilometry (PDV Profilometry) are presented. Although the tradeoff between spatial and temporal resolution still exists with these techniques, their respective strengths and ability to be used concurrently makes them highly useful and a complement to one another.

To show the capabilities of these two measurement techniques two experiments will be performed. Both experiments will utilize a 0.5mm thick 2024-T3 aluminum flyer plate, which will be driven to about twice the speed of sound by a chemically augmented laser impulse (Thurston et al., 2023). This flyer plate was 25mm square. In **Experiment 1** the aluminum flyer plate will be used to induce an impact shock wave in a transparent acrylic cube (25mm on each side). The shock wave will be recorded by the high-speed camera at 10 million frames per second (Shimadzu Hypervision HPV-X2). The properties of this shockwave will then be analyzed. In **Experiment 2** both PDV Profilometry and the high-speed camera will be used simultaneously to capture the changing velocity and profile of the aluminum flyer plate in flight. The high temporal resolution of the PDV Profilometry technique will be shown to complement the comparatively slow high-speed camera by capturing inter-frame flyer profile velocities with a much higher temporal resolution.

To drive the flyer plate used in both experiments an Augmented Laser Impact (ALI) process was used (Thurston et al., 2023). Previously, high intensity pressure pulses have been generated by laser shock for use in laser impact welding and laser shot peening (Thurston et al., 2023). While powerful, laser pulses have limitations when it comes to driving metallic flyer sheets thicker than about 0.25mm (Thurston et al., 2023). Energy may be added to these laser pulses via chemical augmentation. The chemical augmentation used in this work is provided by a mixture known as Gunpowder Nitromethane (GPN) (Abdelmaola et al., 2025). The GPN mixture used here consisted of 10g of 95% purity nitromethane and 1g of smokeless pistol powder. The chemical energy contained in the GPN mixture provides the majority of the energy needed to drive the 0.5mm thick flyer plate used in this work to useful speeds. A commercial laser system with a 3J 8ns pulse (Powerlite TM Precision II Scientific System from Continuum Lasers, Milpitas, CA, USA) was utilized to uniformly detonate the GPN mixture with a laser spot size of 5.22mm. The parameters of the laser system can be found in Table 1.

Power Density (GW/cm^2)	Energy (J)	Wavelength (nm)	Pulse Width (nm)	Spot Size (mm)
1.34	3.14	1064	8	5.22

Table 1: *The parameters of the Laser system*

To make efficient use of the pressure generated by the GPN detonation it is necessary to have the liquid GPN confined between the flyer plate and a transparent tamping medium. The tamping medium's mass and inertia direct the pressure pulse into the flyer plate, thereby making efficient use of the detonation pressure. When laser impulses are used to detonate the GPN the tamping medium must be transparent, therefor in **Experiments 1 & 2** a borosilicate glass tamping layer is used. For this work the borosilicate glass tamper was 9mm thick and was roughly 25x25mm square. This tamper can be seen in **Figure 1A**. Because GPN is a liquid, it must be contained by some method that prevents it from leaking out of the experimental setup and which sets the layer thickness of the GPN. In this work layers of double-sided tape are used at the periphery of the GPN layer to both confine it and to set the layer thickness. Here 4 layers of Scotch brand double sided tape were used. The GPN layer thickness defined by these tape layers was 0.37mm, a layer thickness found to offer the greatest performance (Thurston et al., 2023). The positions of the tamping layer, flyer, and GPN layer are depicted in **Figure 1A**.

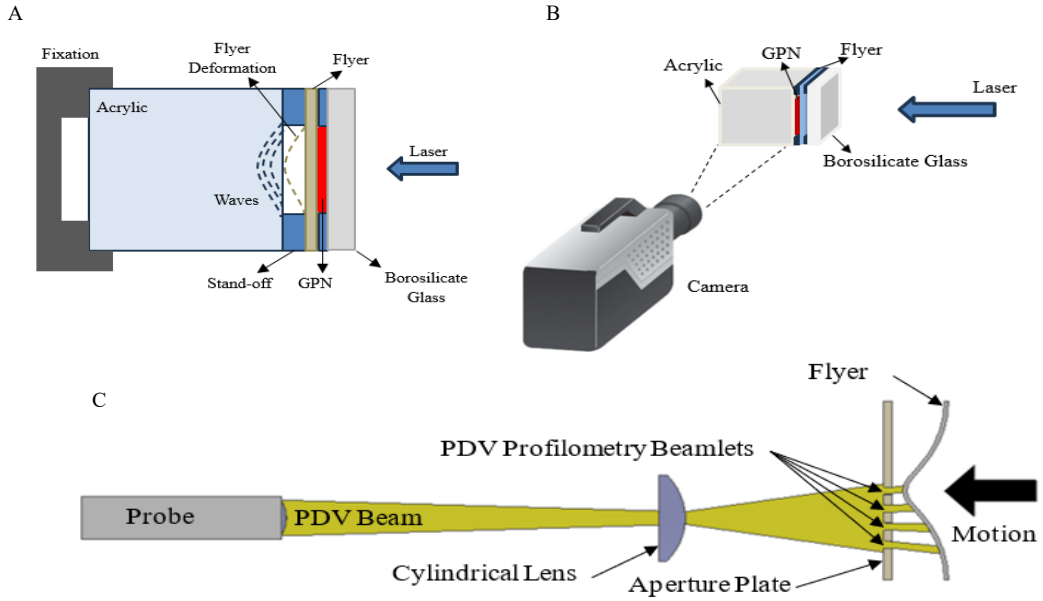

Figure 1: *The setups for both* ***Experiment 1*** *and* ***Experiment 2*** *are shown. A: The schematic of the setup for* ***Experiment 1*** *showing the deformation of the flyer and the shock wave propagation after the flyer collides with the acrylic cube. The location of the GPN augmentation layer and the borosilicate glass tamping layer are shown. The direction of the laser pulse is also indicated. B: The High-Speed Camera configuration used to record* ***Experiments 1 & 2****. C: The setup for PDV Profilometry in* ***Experiment 2****. This setup for* ***Experiment 2*** *is identical to the setup for* ***Experiment 1****, with the exception that the acrylic is replaced by the cylindrical lens and aperture plate.*

The setup for **Experiment 1** is most clearly depicted in **Figure 1A**. As stated previously, this experiment will capture shock propagation in an acrylic cube. As depicted in **Figure 1A**, the 25mm square, 0.5mm thick, 2024-T3 aluminum flyer will be driven toward the acrylic cube by a GPN augmented laser pulse. The aluminum flyer will travel through a standoff gap of 2mm before colliding with the surface of the acrylic cube. At high enough impact speeds a shock wave will be induced in the acrylic. Since the acrylic is transparent it should be possible to observe shock wave propagation with the use of the high-speed camera. As depicted in **Figure 1B**, the high-speed camera will be placed perpendicular

to the direction of flyer motion where it will have a clear view of both flyer motion and shock propagation in the acrylic cube.

Experiment 2 will involve almost the same setup as **Experiment 1**, with the exception that the acrylic cube will be replaced by hardware needed for PDV Profilometry. Typically PDV makes use of a single probe to measure the velocity of a surface by measuring the frequency of a beat frequency created by mixing of a source laser beam and light reflected from the moving surface in question. This beat frequency can be recorded by an oscilloscope and is directly proportional to the velocity of the surface under investigation (Strand et al., 2006). PDV Profilometry takes advantage of the fact that modern signal processing techniques (such as the moving window Fourier transform) can be used to extract multiple beat frequencies from a single PDV signal. As depicted in **Figure 1C**, a single PDV beam may be spread out and divided into individual beamlets by the combination of a cylindrical lens and an aperture plate. So long as the velocity of the flyer under each beamlet is different, the signal recorded on the oscilloscope will contain different beat frequencies for each beamlet. Similarly, because each beamlet has a width, a band of beat frequencies will be generated if a difference in flyer velocity exists across the beamlet. In **Figure 1C** the aperture plate is shown exposing points along the radius of the flyer, therefore ensuring that beamlet should cover a portion of the flyer with a different velocity. In **Experiment 2** the same flyer from Experiment 1 will be recorded moving through free space by both the high-speed camera and PDV Profilometry. The velocity signals from PDV Profilometry will be integrated over time to provide displacement curves that can be compared against measurements from the high-speed camera.

2 Experiment 1 Results and Analysis

This work for Experiment 1 is expected to appear in an upcoming publication by M. Abdelmaola. **Figure 2** provides a sample of frames taken by the high-speed camera of the impact between the aluminum flyer and acrylic, as well as of the shock wave induced in the acrylic.

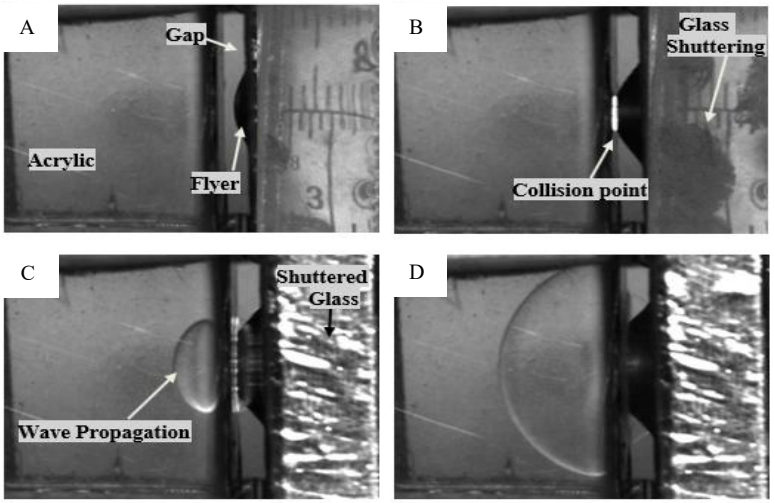

Figure 2: *A: Flyer deformation after the detonation of GPN. B: Collision with target. Here the flyer was traveling 740m/s at impact. C & D: Wave propagation through the acrylic.*

A direct measurement of the shock wave velocity was taken by measuring the change in position of the shock wave between frames as it traveled outward. These measurements

were taken at the central, left most point, of the shock wave. The velocity of the shockwave over time is shown in Figure 3. The peak shock speed velocity shown in Figure 3 is 3428m/s. As should be expected, the shock speed appears to asymptotically fall toward the speed of sound in acrylic, 2,750m/s (Hydrosight GmbH). While the high-speed camera can capture an impressive 10 million frames per second, the velocity of the shock wave when measured by the high speed camera shows unrealistic deviations in velocity. These deviations are due to the relatively course resolution of this camera at 10 million frames per second (200x125 pixels).

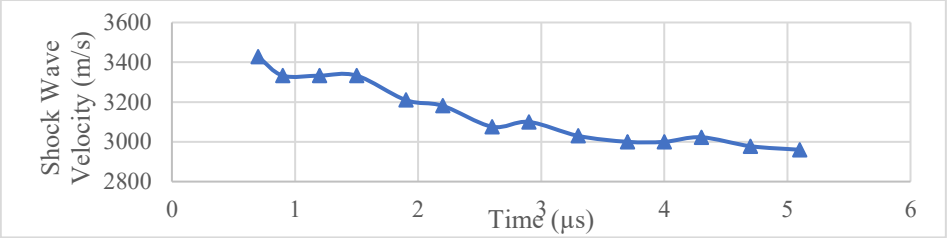

Figure 3: *Shock Wave velocity plotted over time for the impact between the aluminum flyer and the acrylic cube. Here time is measured from the moment of contact. The shock wave does not come into view until 700ns after impact.*

Based on the shock velocity over time curve, and with the equation for shock pressure, $P_2 = P_1 + \rho U_s U_p$ (Marsh, 1980), it is possible to generate a pressure vs time plot for the shockwave traveling within the acrylic cube. Here, P_1 represents atmospheric pressure ($P_1 \approx 0$ for high-speed impact), ρ is the density of the target material (1,190kg/m^3 for acrylic (Hydrosight GmbH)), U_s is the shock wave velocity, and U_p is the particle velocity. P_2 is the pressure behind the wave front, or shock pressure. The particle velocity U_p can be derived from the following equation: $U_p = (U_s - C_0)/(1 + (U_s - C_0)/C_0)$ (Marsh, 1980), where C_0 indicates the speed of sound through the target material (2,720m/s for acrylic). From these equations and the previously plotted shock wave velocity, the shock pressure over time was calculated and then plotted in **Figure 4**.

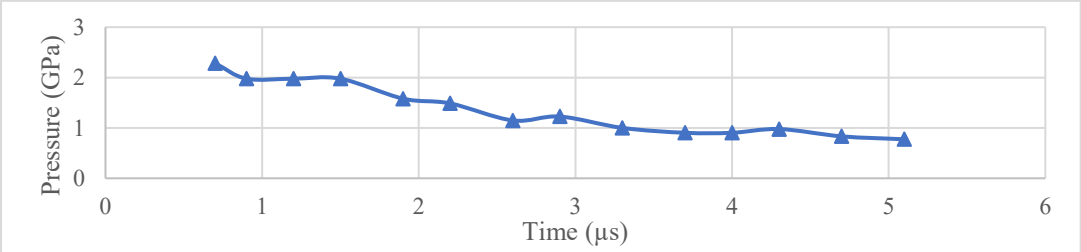

Figure 4: *Pressure behind the wave front after the impact between the aluminum flyer traveling at 740m/s and the acrylic cube. Here time is measured from the moment of contact. The shock wave does not come into view until 700ns after impact.*

3 Experiment 2 Results and Analysis

The work for **Experiment 2** originally appeared in a PhD dissertation by Thurston (Thurston, 2023). The PDV Profilometry data for **Experiment 2** was collected alongside use of the high-speed video camera. The combined beat frequencies from the return light from each of the beamlets was collected and passed through a moving window Fourier transform. The resulting spectrogram can be seen in **Figure 5**. In **Figure 5**, four clear signal bands can

be seen. The top signal is from the beamlet over the center of the flyer. The next three signal bands down are from the three beamlets adjacent to the centermost beamlet. A fifth partial signal band from the furthest radial hole in the aperture plate can also be seen.

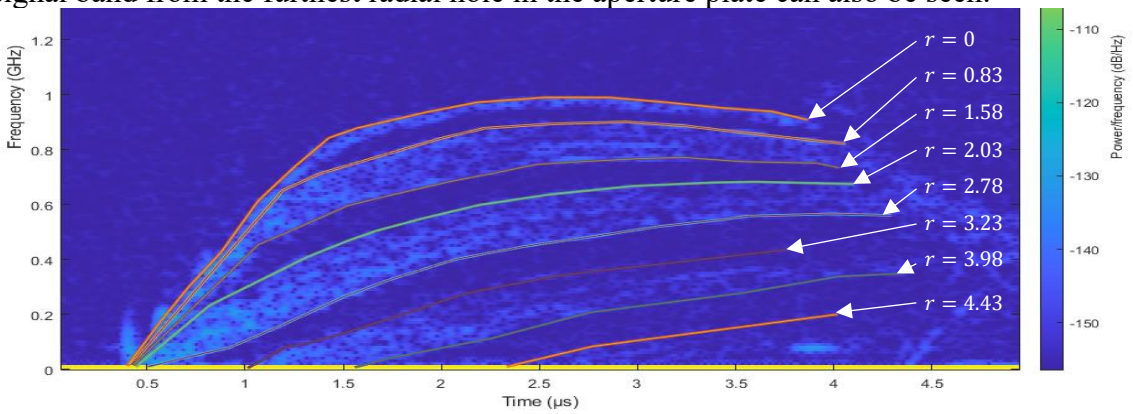

Figure 5: *Spectrogram with PDV Profilometry velocity lines digitized. The radial positions of each line are indicated. The values are in mm.*

The spectrogram in **Figure 5** presents both digitized flyer velocity profiles and the original frequency intensity over time. This spectrogram has a time resolution of 10ns, however the actual time resolution of the spectrogram will vary with the returned frequency, spectrogram calculation parameters, and returned signal intensity. Here the actual time resolution is clearly on the order of 100ns or better. The solid lines on the spectrogram in **Figure 5** are manually digitized representations of the tops and bottoms of the signal bands, which represent the inner and outer edges of each beamlet. This is with the exception of the central beamlet where only the top is digitized, and the fifth partial signal band, for the fifth beamlet, which is only partly present. The central beamlet, which is over the center of the flyer and therefore will have the greatest velocity, is partially digitized because the left and right edges of the beamlet are adjacent to the center of the flyer. Because the locations of the holes in the aperture plate are known it is possible to correlate each of the lines in the **Figure 5** spectrogram with a particular radial coordinate on the surface of the flyer. These radial coordinates are indicated in **Figure 5**. As previously mentioned, the frequencies seen in the spectrogram can be directly converted into velocities, and these velocities can be integrated to produce curves for displacement over time. Because multiple displacement curves are available, and because each displacement curve corresponds to a different radial position on the flyer, it is possible to reconstruct the shape evolution of the flyer over time.

The shape evolution reconstruction of the flyer is shown in **Figure 6**. The PDV Profilometry data has been reflected across the X axis for better visualization.

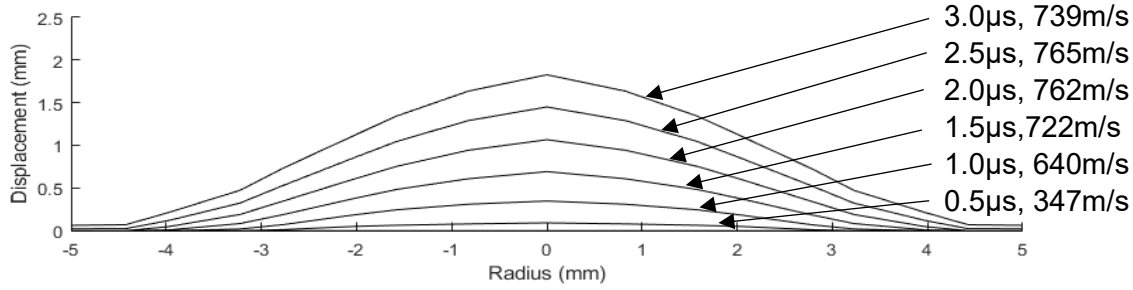

Figure 6: *Reconstructed flyer displacement with flyer tip speed indicated.*

While the data is represented in **Figure 6** is presented as discrete profiles in steps of 0.5μs it should be noted that the actual PDV Profilometry data has a time resolution in the

tens of nanoseconds or less. The last profile given in **Figure 6**, at 3.0µs, has a displacement approaching 2mm, the same as the standoff distance between the flyer and the acrylic cube in **Experiment 1**.

In an effort to compare the strengths and weaknesses of the high-speed camera and PDV Profilometry an unconstrained flyer was filmed under the same conditions as the flyer used to collect the PDV Profilometry data, with the exception that the aperture plate was removed. In **Figure 7** several frames collected by the high-speed camera from this flyer are presented at intervals of 0.5µs. The shape evolution of the flyer shown in these images superficially resembles the shape evolution reconstructed from the PDV Profilometry data presented in **Figure 6**. In order to make a more accurate comparison between the PDV Profilometry data and the high-speed camera data a MATLAB script was written to extract the leading edge of the flyer profiles from the high-speed camera images.

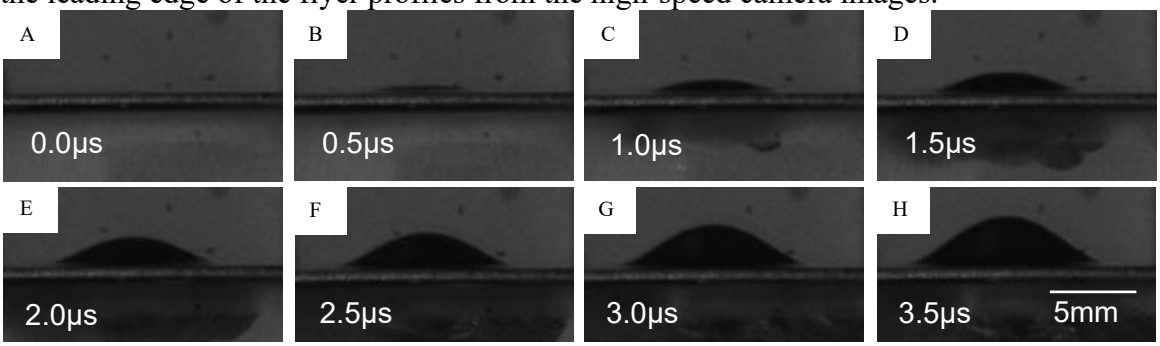

Figure 7: *Frames collected by the high-speed camera.*

As can be seen in **Figure 8**, the PDV Profilometry data compares well to the flyer profiles generated from the high-speed camera footage. In **Figure 8** the high-speed camera flyer profiles are shown overtop of the PDV Profilometry profiles for better comparison. The regions of the flyer away from the center point show greater displacement in the high-speed camera profiles as compared to the PDV Profilometry derived profiles. This may be due to shot-to-shot variability in the Augmented Laser Impact process, or calibration issues with the scaling of the high-speed images. For better comparison PDV Profilometry and high-speed photography should be done on the same experiment. This was not done here due to time constraints with the high-speed camera.

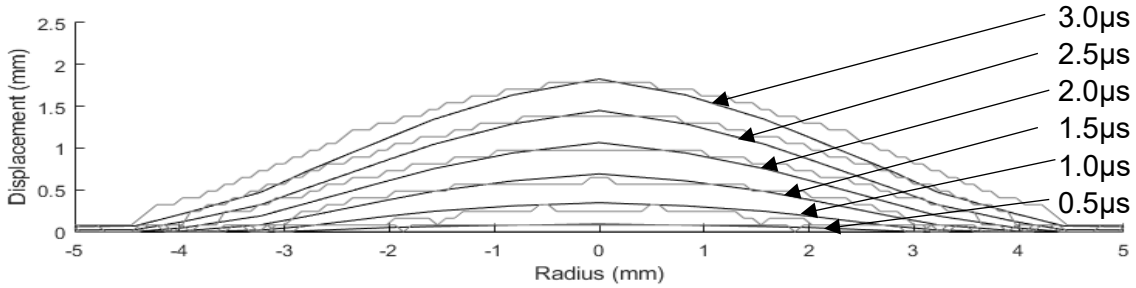

Figure 8: *High-speed camera flyer profiles overlaid on PDV Profilometry data.*

4 Conclusions

In this work two techniques or data acquisition at high speeds were presented. The high-speed camera was shown to offer great spatial resolution, along with a time resolution of 10 million frames per second. It was shown that for transparent media the high-speed

camera can be used to measure shock wave velocities. From those shock wave velocities, it is possible to calculate shock pressures in the transparent media as a function of time. PDV Profilometry showed that adaptations to the standard PDV technique can allow for easy extraction of flyer velocity profiles, and by integration, flyer displacement profiles over time can also be gathered. PDV Profilometry velocity and displacement data can have a tremendously high time resolution as compared to even the best high-speed cameras. Here the time resolution of the PDV Profilometry data was better than 100ns, ten times faster than the high-speed camera. Although the spatial resolution of PDV Profilometry is somewhat lacking. PDV and PDV Profilometry serve as a complement to the high-speed camera both as a means of cross validation, and as a means of measuring velocity data directly at a much higher time resolution. It is hoped that future researchers will see the utility in these data acquisition techniques for short duration and high velocity experiments.

References

D. B. Watts and M. T. Van Tassel, 'Transducer Development for Explosive Measurements', Instrumentation Technology Branch Advanced Guidance Division, Florida, 1989.

L. Elkarous, C. Robbe, M. Pirlot, and J.-C. Golinval, 'Dynamic calibration of piezoelectric transducers for ballistic high-pressure measurement', Int. J. Metrol. Qual. Eng., vol. 7, no. 2, Art. no. 2, 2016, doi: 10.1051/ijmqe/2016004.

B. Thurston, T. Lewis, J. Li, A. Vivek, and G. Daehn, 'Augmented Laser Impact Welding: A New Process Demonstration in Welding Aluminum Alloy 2024-T3', Journal of Materials Engineering and Performance, Oct. 2023, doi: 10.1007/s11665-023-08808-2.

M. Abdelmaola, B. Thurston, B. Panton, A. Vivek, and G. Daehn, 'Influence of Augmentation Compositions and Confinement Layers on Flyer Velocity in Laser Impact Welding', Metals, vol. 15, no. 2, Art. no. 2, Feb. 2025, doi: 10.3390/met15020190.

Strand, O. T., Goosman, D. R., Martinez, C., Whitworth, T. L., & Kuhlow, W. W. (2006). Compact system for high-speed velocimetry using heterodyne techniques. Review of Scientific Instruments, 77(8), 083108.

Hydrosight GmbH, https://www.hydrosight.com/acrylic-vs-polycarbonate-a-quantitative-and-qualitative-comparison

S. P. Marsh, LASL shock hugoniot data / Stanley P. Marsh, editor. in Los Alamos series on dynamic material properties. Berkeley, Calif: University of California Press, 1980.

Thurston, B. P. (2023). Developments in Advanced Manufacturing Techniques: Impact Welding and Metamorphic Manufacturing [Doctoral dissertation, Ohio State University]. OhioLINK Electronic Theses and Dissertations Center. http://rave.ohiolink.edu/etdc/view?acc_num=osu1689951299143669